We are IntechOpen,
the world's leading publisher of
Open Access books
Built by scientists, for scientists

6,900
Open access books available

185,000
International authors and editors

200M
Downloads

154
Countries delivered to

Our authors are among the

TOP 1%
most cited scientists

12.2%
Contributors from top 500 universities

WEB OF SCIENCE™

Selection of our books indexed in the Book Citation Index
in Web of Science™ Core Collection (BKCI)

Interested in publishing with us?
Contact book.department@intechopen.com

Numbers displayed above are based on latest data collected.
For more information visit www.intechopen.com

Ultrasound for Membrane Fouling Control in Wastewater Treatment and Protein Purification Downstream Processing Applications

Amira Abdelrasoul and Huu Doan

Abstract

Membrane fouling is one of the major issues encountered in membrane filtration including microfiltration, ultrafiltration, nanofiltration, and reverse osmosis. Membrane fouling can occur due to the reversible and irreversible deposition of particles, colloids, macromolecules, salts, and other types of elements. As a consequence, fouling causes a significant decrease in the permeate flux due to plugging of membrane pores, and adsorption of fouling material on the membrane's surface and/or in the pore walls. A lot of research efforts have been directed towards fouling remediation techniques or membrane cleaning alternatives. Although most of these methods are relatively functional, they have drawbacks and limitations. Among these methods, the use of ultrasound has been shown to be effective in enhancing mass transfer, cleaning, disinfection, and controlling fouling. In membrane filtration processes, ultrasound can help accelerating the permeate flux towards the membrane and decreasing the concentration of solutes accumulated in the membrane pores and on the membrane surfaces. Ultrasonic fouling control does not require chemical cleaning and can maintain a high permeate flux throughout the filtration process. In addition, wastewater contaminants can be degraded by ultrasound. Therefore, ultrasound creates unique physicochemical conditions, which can be used as an effective tool for membrane fouling control. In this chapter, ultrasound radiation as a unique method to modify physical and chemical properties of a complex fluid with applications in wastewater treatment and protein purification process is highlighted. At first, ultrasonic parameters and how their ability to enhance the delivery of fluid flow to the membrane surface and affect the physical and chemical properties of foulants are discussed. Furthermore, various ultrasonic methods, including continuous and intermittent waves, and its influences on membrane fouling, permeate flux, membrane cleaning and flux recovery are reviewed. The main role of wave streaming as a driving force for fluid acceleration and antifouling control, and the impact of ultrasound-generated bubble cavitation on preventing and removing fouling deposits are described. The challenges of current ultrasonic techniques, which need to be addressed so as to facilitate their widespread and successful implementation, are explored. This chapter examines how the periodic compression/rarefaction cycles of ultrasound can influence mass transfer and membrane fouling. Also, the current knowledge and approaches to advance ultrasonic technology as an

effective method for membrane fouling remediation in wastewater treatment and protein purification downstream processing are presented in this chapter.

1. Overview of membrane fouling mechanisms

Membrane processes are increasingly used in various applications, both upstream and downstream processes, such as microfiltration (MF), ultrafiltration (UF), and emerging processes including membrane chromatography, high performance tangential flow filtration, and electrophoretic membrane contactor. Membrane fouling is an ongoing issue in pressure-driven membrane processes such as UF, MF, nanofiltration (NF), reverse osmosis (RO), and forward osmosis (FO). Membrane fouling is likewise unavoidable in other types of membrane-based processes such as membrane distillation (MD) and membrane bioreactor (MBR). In recent years, the application of UF has expanded as a promising alternative technology to obtain drinking water [1–4]. In addition, UF has become particularly important in concentrating proteinaceous solutions. Examples of commercial membrane processes include filtration of protein solutions in the presence of electrolytes, concentration of whey proteins in the dairy industry, protein recovery from blood plasma, and protein concentration in downstream processing. NF is another promising technology that separates solutes based on solute charge and size. Several research papers on peptide fractionation by NF of model systems of amino acids and peptides, which were based on molecular sieve effect and/or on charge effect depending on the membrane type and the feed phase composition, have been reported [5]. However, one of the major factors, which hinders more wide-spread applications of membrane filtration, is that the permeate flux declines with filtration time [6–9]. This phenomenon is commonly known as membrane fouling, which refers to the blockage of membrane pores by the combination of sieving and adsorption of particulates and compounds onto the membrane surface or within the membrane pores during the filtration process, as summarized in **Figure 1**.

In-depth understanding of fouling phenomenon mechanisms is vital for the advancement of innovative methods for the control of fouling and cleaning of membranes. Membrane fouling is a complex process since it involves chemical and physical interactions between various foulants as well as between the membrane's surface and foulants [10–12]. Membrane fouling reduces the active area of the membrane, blocks the membrane pores, or increases the resistance to the flow though the membrane and hence directly contributes to a declined in the permeate flux and an increased transmembrane pressure, which in turn results in an increase in the power consumption [13, 14]. Membrane fouling presents in the form of pore blockage, particle deposition, adsorption, or gel formation, as shown in **Figure 1**. Adsorption of contaminants on the membrane surface, due to interactions between foulants and the membrane surface, and the membrane's pore walls produces higher hydraulic resistance across the membrane. Alternatively, pore blockage is comprised of the plugging of the membrane's pores that in turn narrows the passage for the permeate through the membrane, resulting in a lower permeate flux [7, 9]. The deposition of foulants by layer-by-layer accumulation on the membrane surface creates additional hydraulic resistance, which is otherwise known as cake resistance [3]. When it comes to fouling caused by the gel formation, the cross-linked three-dimensional networks of deposited particles, including colloidal substances and macromolecules, are created on the surface of the membrane. These formed gel
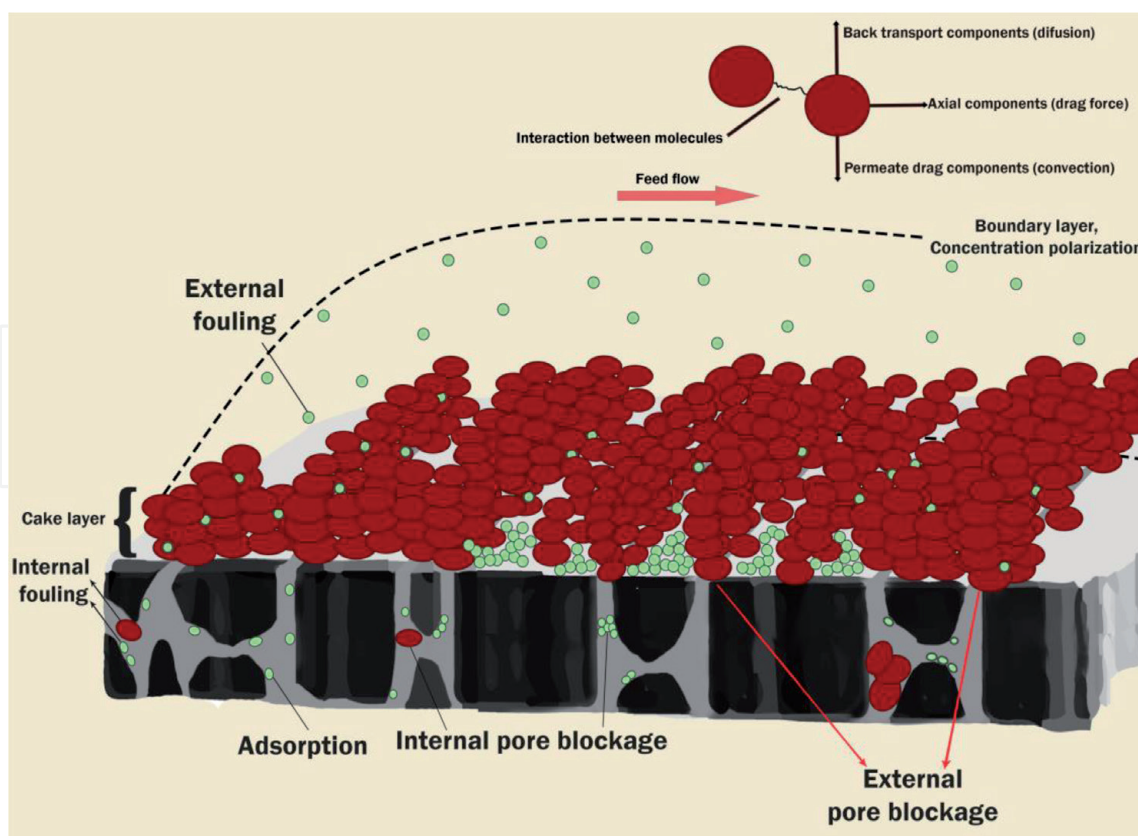
Figure 1.
Membrane fouling mechanisms.

layers lack connectivity between the pores and as a consequence offer greater resistance to mass transport through the membrane. Once the gel layer is formed, any increase in the transmembrane pressure will not result in any improvement in the permeate flux, but it will compress the gel layer [3, 4]. Deposition of foulants on the membrane's surface is generally known as external fouling, whereas fouling within the membrane's pores is defined as internal fouling, as shown in **Figure 1**. In most cases, the process of flux decline transpires in three specific stages due to the fouling mechanisms. During Stage I, there is a rapid flux decrease because of the swift pore blocking happening at the beginning of the process. During Stage II, the flux continues to decrease due to the cake layer formation and consequent growth. In this stage, the flux continues declining, while the cake layer increases and attains greater thickness. During Stage III, the fouling process gets to a relatively steady state, and the cake layer grows to its equilibrium thickness [3, 11, 12, 14]. The change from the initial flux to the steady-state flux may be quite substantial. Diverse foulant types can occur in membrane-based separation processes, dependent on the properties of the feed stream. Membrane fouling can thus be classified based on the foulant types [4, 13]. In this chapter, ultrasound radiation as a unique method to modify physical and chemical properties of a complex fluid with applications in wastewater treatment and protein purification process is highlighted.

1.1 Types of fouling

1.1.1 Organic fouling

The presence of the organic fouling is frequent in the membrane-based separation processes because of the pervasive occurrence of dissolved organic matter (DOM) in wastewater, sewage, and surface water. DOM can be classified into three

key categories: (1) natural organic matter (NOM), created through metabolic reactions of organics in various sources of drinking water; (2) synthetic organic compounds (SOC), discharged into wastewater streams and originating from industries and household sources; and (3) soluble microbial products (SMP), produced during biological water treatment processes [15]. When it comes to NOM, the primary constituents in ground or surface waters are humic substances (fulvic acids, humic acids, and humin) created through the decomposition of animal and plant residues. As such, humic substances include aliphatic and aromatic constituents of phenolic and carboxylic functional groups. Furthermore, NOM encompasses nonhumic fractions that are based on amino acids, proteins, transphilic acids, and carbohydrates [16]. There are several mechanisms in which NOM can create organic fouling. NOM may form a gel layer on the membrane surface, be adsorbed or deposited within the membrane pores, or bind to other particles in order to form a NOM/particle fouling layer on the membrane surface. Organic fouling could likewise be produced by transparent exopolymer particles (TEPs) created from polysaccharides and excreted by microalgae [17]. Furthermore, effluent organic matter (EfOM), consisting of SMP and NOM, from biological wastewater treatment may become the source of membrane's organic fouling. EfOM could include compounds including enzymes, nucleic acids, antibiotics, polysaccharides, proteins, and steroids [17]. In general, organic membrane fouling is a complicated phenomenon that is directly influenced by the foulant-membrane surface interactions, foulant-foulant interactions, and feed water's chemistry. For the initial buildup of organic fouling layer, adsorption is a key mechanism, which is responsible for irreversible fouling. It should also be noted that the hydrophilicity or hydrophobicity and molecular size of NOM have a critical role in the formation of the membrane's organic fouling and flux decline [18].

1.1.2 Inorganic fouling

Inorganic membrane fouling is frequently referred to as "mineral scaling." This type of fouling is caused by the elevated concentrations of inorganic compounds in the feed water. Examples of inorganic foulants are calcium carbonate ($CaCO_3$), barium sulfate ($BaSO_4$), calcium sulfate ($CaSO_4$), and silica (SiO_2). The primary cationic species that are responsible for inorganic fouling are Mg^{+2}, Fe^{+3}, Ca^{+2}, and Al^{+3}. Alternatively, the primary inorganic species that can be in equilibrium with cationic scaling components are F^-, CO_3^{-2}, SO_4^{-2}, OH^-, silicic acids, and orthophosphate [19]. The scale formation or inorganic fouling on the membrane surface is controlled by transport and crystallization mechanisms. Crystallization can happen as a consequence of ion precipitation on the membrane surface. This occurs when the overall ion activity in the feed water is above the saturation limit, a dynamic where the feed is essentially supersaturated. Scaling caused by crystallization can occur in two potential ways: surface (heterogeneous) crystallization and bulk (homogeneous) crystallization. During bulk crystallization, the crystal particles deposit on the membrane surface and then create a cake layer, after being formed through homogeneous crystallization in the bulk phase. Supersaturated solutes permit the agglomeration of scale-forming ions because of the random collisions occurring in the bulk phase. The coalescing ion cluster facilitates precipitation once it becomes larger than a critical size. For surface crystallization, the crystals are formed on the membrane surface, while the scale formation occurs through the lateral crystal growth [19]. Inorganic fouling can be influenced by several parameters, including degree of super saturation, shear across the membrane, transmembrane pressure, membrane surface roughness, and the feed solution chemistry [20]. Membranes that have rougher surfaces are more susceptible to inorganic fouling than those featuring smoother surfaces. Greater surface roughness augments free energy on the surface

and in turn raises membrane's adhesiveness. Inorganic fouling is more frequent at low-shear rates, higher degrees of super saturation, and higher transmembrane pressure. Furthermore, inorganic fouling can become more aggressive in cases where the wastewater contains smaller particles and greater concentrations.

1.1.3 Colloidal fouling

Common examples of inorganic colloids are colloidal silica, elemental sulfur, precipitated iron, silt, aluminum silicate clays, and corrosion products. Alternatively, organic colloids can be carbohydrates, proteins, fats, oils, and greases. During membrane filtration process, permeate flux is the primary mechanism for the transportation of colloidal particulates from the bulk feed to the membrane surface. Simultaneously, cross flow prompts reverse transport of colloids from the membrane surface to the bulk feed. Reverse transport of colloids is generally controlled by turbulent transport, particle rolling, inertial-lift forces, Brownian diffusion, shear-induced diffusion, and particle-particle interaction forces [11]. For nonporous membranes such as NF or RO, colloidal fouling is triggered by the buildup of particles on the membrane surface that causes the cake layer formation. For porous membranes, including UF and MF, the pore size is large enough so as to facilitate pore blocking; hence, colloidal fouling can be caused by surface accumulation and pore plugging [13]. The surface charge and physiochemical properties of colloids depend on the feed solution chemistry, such as pH, ionic composition, and ionic strength [21]. Furthermore, colloidal fouling depends on other membrane properties. Smoother and more hydrophilic membranes exhibit superior colloidal fouling resistance potential during the initial fouling stage [11, 21]. Colloidal fouling likewise relies on the hydrodynamic conditions, that is, the fouling becomes more problematic at lower cross-flow velocity [21].

1.1.4 Biofouling

Biofouling is caused by the deposition, growth, and metabolism of microbiological cells (bacteria, algae, protozoa, and fungi) or flocs, in conjunction with the production of biofilm on the membrane. Biofouling poses a serious operational problem in membrane-based processes and is a contributing factor to >45% of all membrane fouling [10]. Biofouling begins as an attachment of microbiological cells to the membrane surface, which then causes the formation of biofilm. After the initial attachment, the microbiological cells continue to grow and multiply by using the feed nutrients and/or the organics adsorbed in the membrane surface as its resources. Simultaneously, the extracellular polymeric substances (EPSs) excrete in a manner that anchors the microbiological cells and allows further settlement on the membrane surface. Once their growth is completed, the cells begin to detach and then diffuse to new locations on the membrane surface so as to once again initiate biofilm creation [22]. The biofilm growth can be summarized as a series of steps: (a) formation of a conditioning film through the absorption of organic species (macromolecules, proteins, etc.) on the membrane surface, (b) transportation of microbiological cells from the bulk feed to the conditioning film, (c) attachment of cells to the membrane surface, and (d) creation of biofilm through cell growth [22]. The process of cell attachment is dependent on the membrane properties, including roughness, hydrophobicity, material, and surface charge. The features of microbiological cells and the properties of feed water influence the attachment of cells to the membrane surface [22]. Furthermore, the EPSs play an important role in biofouling. EPS substances tend to be higher molecular weight secretions of the microbiological cells, such as proteins, nucleic acids, polysaccharides, and lipids. EPSs are distinguished as

soluble EPS (or SMP) and bound EPS. Bound EPSs are sturdily bound to the micro-biological cells, meanwhile the soluble EPSs are loosely bound and appear primarily in the form of dissolved substances in the bulk liquid. EPSs contain hydrophobic and hydrophilic functional groups that allow them to be positioned on hydrophobic and hydrophilic membranes. EPSs offer a way to bind the cells together in three-dimensional matrices. As such, EPS can influence the biofilm's structural stability, adhesion ability, surface parameters, and stability of the microbiological cells [22].

Fouling can be reduced by manipulating particle-to-membrane and particle-to-particle interactions. For this purpose, a wide variety of feed pre-treatment options can be used. However, this can rapidly increase operational cost and complexity [1–3]. Chemical cleaning consists of the use of acid, alkali, or biocide solution to prevent inorganic fouling, organic fouling, and biofouling, respectively. Almost full recovery of permeate flux can be achieved through chemical cleaning; however, it can increase cost and complexity of filtration process due to the use of hazardous chemicals. Furthermore, it produces by-products that are threatening to the environment. Physical cleaning includes periodic rinsing (backwashing and flushing), which consists of passing water through the membrane in the reverse direction of the permeate flux. Backwash with air can also be applied to remove particles through surface shear and increase in mass transferring motion, but it is not compatible to all types of feed solution [7–10]. Another physical technique is the use of pulsed electric or ultrasonic fields during the filtration process to avoid particle deposition [7, 8]. As an alternative to these techniques, the use of ultrasonic field in membrane cleaning and fouling control has been investigated. Ultrasound (US) can create turbulence near the membrane surface and detach particles through the action of cavitation bubbles. The characteristics of the bubbles formed within the system play a major role in the effectiveness of the ultrasound application. The particle detachment can significantly decrease the overall resistance to flow across the membrane, increasing the filtration performance.

2. Theoretical aspects of ultrasound membrane fouling control

The ultrasound influence on membrane fouling control is function of wave parameters, time, the fluid characteristics, pressure, and temperature.

2.1 Ultrasound phenomenon

Ultrasound is a sound (acoustic) wave traveling at a frequency greater than 20 kHz, which is above the normal human hearing range [23]. Unlike the audible sound range, ultrasound has exceptional chemical and physical properties by transmitting high mechanical power through small mechanical movements [24]. As shown in **Figure 2**, ultrasound spreads through a fluid in a series of rarefaction (expansion) and compression waves. Because of this propagation, the molecules within the fluid are exposed to rarefaction and compression cycles in the direction of the wave propagation. This generates an acoustic pressure (P_a) in addition to the fluid's hydrostatic pressure (P_0). The acoustic pressure generated can be calculated using Eq. (1) [24]:

$$P_a = P_A \sin(2\pi f t) \tag{1}$$

where P_A, f, and t stand for the acoustic pressure amplitude, frequency, and time, respectively.

Three distinctive types of ultrasound are classified based on the sound frequency range, specifically power ultrasound (20–100 kHz), high frequency ultrasound (100 kHz–1 MHz), and diagnostic ultrasound (1–500 MHz) [26].
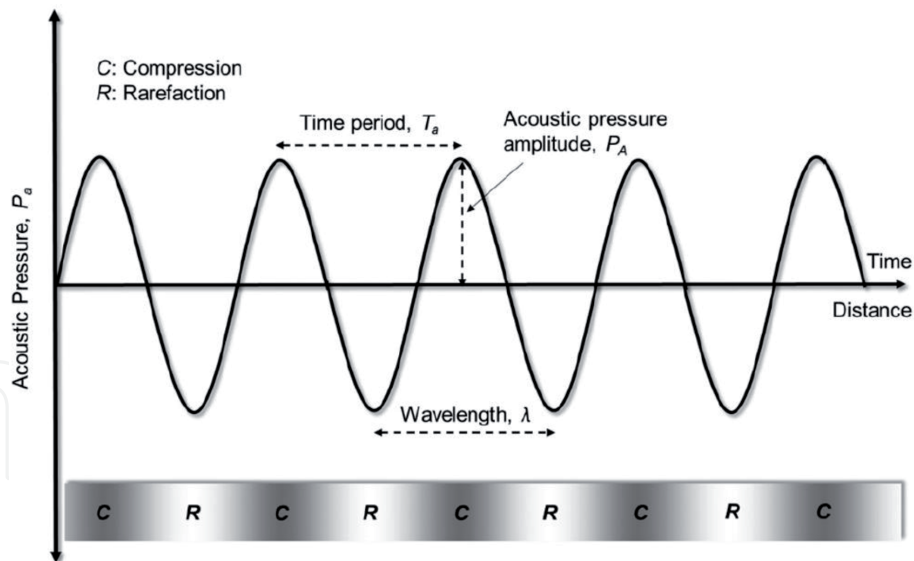
Figure 2.
Schematic diagram of an ultrasonic wave [25].

For processing and industrial cleaning applications, the ultrasound frequency range between 20 and 500 kHz is usually used [26].

2.2 Acoustic cavitation

In the compression cycle, the molecules in the fluid are exposed to a positive acoustic pressure that pushes the molecules closer to one another. Alternatively, in the rarefaction cycle, a negative pressure is applied in order to pull the molecules away from each other. The intermolecular forces are incapable of holding the molecules together, and small vapor-filled voids, or cavitation bubbles, are formed in the liquid whenever the pressure amplitude and the subsequent tensile stress during rarefaction are greater than the tensile strength of the liquid [27]. This phenomenon is known as the acoustic cavitation. The minimum acoustic pressure necessary to transcend the liquid tensile strength and form a cavitation bubble of an initial radius R_0 is termed the Blake threshold (P_b) and is defined by Eq. (2) [27]:

$$P_b = P_o + 2/3 \sqrt{\frac{(2\sigma/R_o)^3}{3\left(P_o + \frac{2\sigma}{R_o}\right)}} \qquad (2)$$

where P_o is the hydrostatic pressure being applied on the liquid, and σ is the liquid's surface tension. In Eq. (2), the expression ($\frac{2\sigma}{R_o}$) signifies the cavitation bubble's surface tension. It should be noted that Eq. (2) does not properly address inertial and viscous effects and vapor pressure [28]. The creation of cavitation bubbles in a liquid is usually linked to the nucleation phenomenon and the existence of weak spots, including solid impurities, dissolved solids, free-floating gas bubbles, and gas pockets in crevices of solids acting as nuclei [25]. Generally, the ultrasound cannot create cavitation bubbles in pure liquids that naturally have excessively high-tensile strength. However, the existence of impurities drastically lowers the liquid's tensile strength and, as a consequence, the required Blake threshold for the initiation of cavitation. For example, the Blake threshold value for impure liquids is around 1–10% of the Blake threshold for pure liquids [27, 28].

2.3 Cavitation bubble growth

After cavitation bubbles are created, they can disperse in liquid and grow larger. The cavitation bubbles grow because of the rectified diffusion and coalescence.

Coalescence is the process during which smaller cavitation bubbles join together to form larger bubbles. On the other hand, rectified diffusion occurs when the bubble growth undergoes repeated rarefaction and compression cycles produced by the ultrasound. During the compression cycle, the bubbles are compressed, while the contained material, such as gases and vapors, is released into the liquid. The quantity of material leaving or entering a bubble is directly proportional to the bubble surface area. In general, the quantity of the expelled material during the compression cycle is less than the amount gained during the rarefaction cycle because of the lower surface area accessible throughout the compression cycle. As a consequence, the bubbles continue to grow in size, while the ultrasonic field is present. Supplemental to the area effect, shell effect likewise needs to be addressed during rectified diffusion [29]. Shell effect is connected to the liquid shell thickness around the cavitation bubbles. In the compression cycle, the bubbles begin to shrink, while the overall thickness of the liquid shell around them is increasing. As a result, there is a decrease in the gas concentration close to the wall of the bubbles. Thus, a lower concentration gradient exists for the gas movement out of the bubbles across thicker liquid shells. In the rarefaction cycle, the bubbles begin to expand, while the overall thickness of the liquid shell becomes thinner. This change incites an increase in gas concentration close to the wall out of bubbles. A high concentration gradient comes with a thin liquid shell on the bubble under rarefaction. In contrast to the compression cycle, a higher quantity of gas travels into the bubbles during the rarefaction cycle. As a result, the overall outcome is the increase in the bubble size. Generally, the bubbles grow to a maximum size of 2–150 μm [25].

2.4 Cavitational collapse

Once the bubbles have grown to a certain size, degassing can happen where the bubbles leave the liquid due to buoyancy. If the bubbles continue growing to a critical size by rectified diffusion, which is designated as the bubble resonance size (R_r), then they can continue fluctuating around the resonance size, or alternatively growing to a larger size at which they collapse [29]. The bubble resonance size is a function of ultrasound frequency and can be estimated using Eq. (3) [28]:

$$R_r = \sqrt{\frac{3\gamma P_o}{\rho\omega^2}} \tag{3}$$

where ω stands for the ultrasonic angular frequency, γ is the specific heat ratio of gas (Cp/Cv, Cp, and Cv are specific heat of gas at constant pressure and constant volume, respectively) within the bubble, and ρ is the liquid density. For air bubbles in water, Eq. (4) [27] can be used to estimate the resonance radius:

$$R_r \approx \frac{3}{f} \tag{4}$$

where f stands for the ultrasound frequency. The collapse of the bubbles, or cavitational collapse, is controlled by the bubble oscillation frequency (f_b) as expressed in Eq. (5) [28]:

$$f_b = \frac{1}{2\pi R}\sqrt{\frac{3\gamma}{\rho}\left(P_o + \frac{2\sigma}{R}\right)} \tag{5}$$

where R represents the bubble radius.

The bubbles remain intact and continue their growth cycle if the resonant bubble oscillation frequency (the bubble radius is at its resonance value) is smaller than the ultrasound frequency at the end of the compression cycle. This particular dynamic is defined as the noninertial, stable, or steady cavitation, during which

the bubbles continue to oscillate over many rarefaction and compression cycles until they grow larger and finally collapse. When the resonant frequency becomes equal to or greater than the ultrasound frequency, the bubbles can grow incredibly fast and then violently collapse into smaller bubbles within a single acoustic cycle [25, 29]. This process is regarded as inertial or transient cavitation and implies that the lifetime of the bubbles is quite short. Transient cavitation happens at high ultrasound intensities, while the stable cavitation usually occurs at low ultrasound intensities. It is relevant to note that stable cavitation may eventually lead to transient cavitation, and transient cavitation may generate smaller bubbles that then experience stable cavitation. **Figure 3** offers a summary of the cavitation bubble growth and the cavitational collapse in an ultrasonic field.

2.5 Dynamics of bubble growth

The radial growth is governed by the Rayleigh-Plesset equation, as presented in Eq. (6) [27]:

$$R\frac{d2R}{dt^2} + \frac{3}{2}\left(\frac{dR}{dt}\right)^2 = \frac{1}{\rho}\left[\left(P_o + \frac{2\sigma}{R_o}\left(\frac{R_o}{R}\right)^{3\gamma} - \frac{2\sigma}{R} - \frac{4\mu}{R}\left(\frac{dR}{dt}\right) - P_\infty\right]\right] \tag{6}$$

where R is the growing bubble's radius, μ is the liquid viscosity, and Po and $P\infty$ are the pressure close to the bubble and pressure at an infinite distance away from the bubble. In the system represented by Eq. (6), liquid is considered incompressible, and the bubble is full of an ideal gas; thus, the system behaves adiabatically. The pressure at an infinite distance from the bubble, P_∞, is dependent on time (t) and can be determined by Eq. (7) [25]:

$$P_\infty = P_o - P_A \sin(\omega t) \tag{7}$$

Equation (8) [29] is applicable for radial growth of a gas-filled transient bubble [30]:

$$R\frac{d2R}{dt^2} + \frac{3}{2}\left(\frac{dR}{dt}\right)^2 = \frac{1}{\rho}\left[P\left(\frac{R_{max}}{R}\right)^{3\gamma} - P_m\right] \tag{8}$$

where R_{max} stands for the maximum bubble radius before the bubble collapse, P is the pressure (as a sum of the gas pressure, P_g, and the vapor pressure, P_v) inside
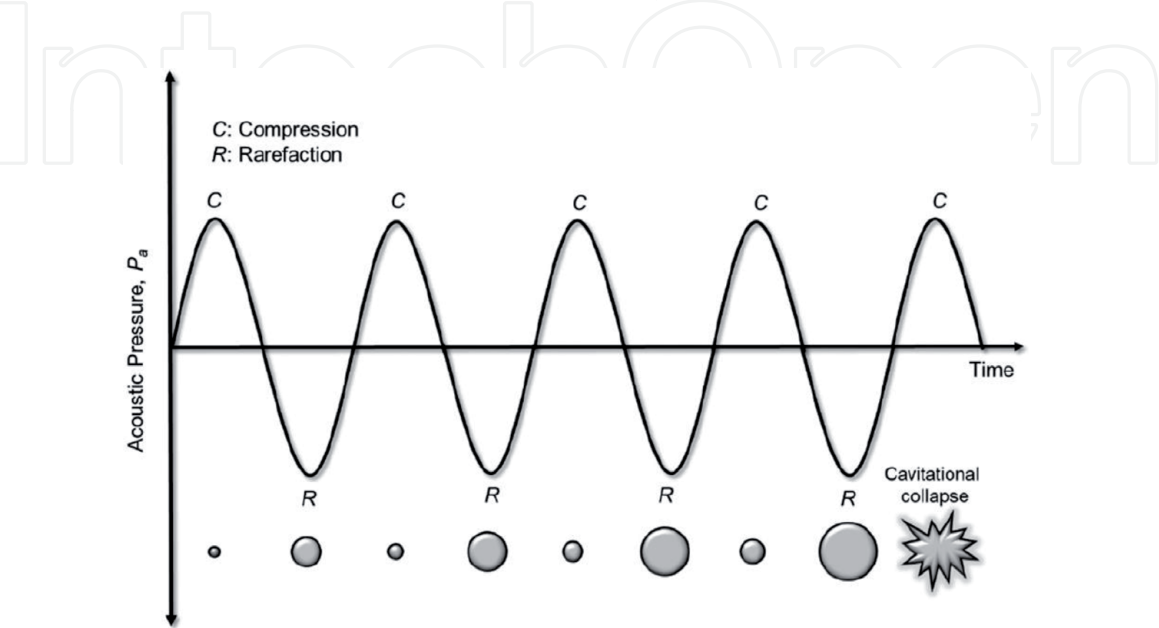

Figure 3.
Schematic diagram of acoustic cavitation, bubble growth, and cavitational collapse [29].

the bubble at the maximum radius value ($P = P_v + P_g$), and P_m is the liquid pressure at the transient collapse moment ($P_m = P_0 + P_A$). The bubble collapse time (τ_m) can be estimated using Eq. (9) [25]:

$$\tau_m = 0.915 R_{max} \left(1 + \frac{P}{P_m}\right) \sqrt{\left(\frac{\rho}{P_m}\right)} \tag{9}$$

2.6 Effects of cavitational collapse

Cavitational collapse generates sonoluminescence, where short light bursts are released [29]. Furthermore, forceful collapse of transient cavitation bubbles may cause significant chemical and mechanical effects in liquid systems due to the concentration of ultrasound energy at the bubble collapse sites. Cavitational collapse creates hotspots with extremely high local pressures and temperatures. Generally, hot spot pressure and temperature can reach up to 1000 atm and 5000 K [31]. The lifetime of a hotspot is rather short, which leads to a very high cooling and heating rate, often surpassing 109 Ks^{-1} [29, 31]. If the gas in a bubble is assumed to be ideal, and the viscosity and surface tension of liquid are ignored, then the maximum pressure (P_{max}) and the maximum temperature (T_{max}) within a collapsing bubble can be calculated using Eqs. (10) and (11) [31]:

$$T_{max} = T_o \left[\frac{P_m}{P}(\gamma - 1)\right] \tag{10}$$

$$P_{max} = P_o \left[\frac{P_m}{P}(\gamma - 1)\right]^{\frac{\gamma}{(\gamma-1)}} \tag{11}$$

where T_o is the ambient temperature.

The local high pressure and temperature conditions at the bubble collapse sites offer locations for high-energy sonochemical reactions that involve free radicals. Such high-energy reactions are usually justified using the "hot spot" model. In this model, there are three specific regions in the presence of sonochemical reactions: (1) a hot gaseous nucleus (thermolytic center), (2) an interfacial region, and (3) the bulk liquid at ambient temperature values [30].

2.7 Factors affecting acoustic cavitation and cavitational collapse in membrane process

There are multiple factors affecting the acoustic cavitation and the subsequent collapse of the cavitation bubbles in an ultrasonic field. Those key factors are examined later.

2.7.1 Ultrasonic frequency and intensity

Lower ultrasound frequency augments the size of the produced cavitation bubbles, thus leading to an intense cavitational collapse. For higher ultrasound frequency values, acoustic cavitation and cavitational collapse are less frequent due to two reasons. First, the negative acoustic pressure during the rarefaction cycle is unable to initiate the cavitation. Second, the compression cycle is much faster and does not provide enough time for the bubbles to collapse [25, 29].

Acoustic cavitation displays an optimal relationship with the ultrasound intensity. The power intensity can be determined calorimetrically or by using the input or output power per unit area of the ultrasound transducer [31]. Ultrasound intensity (I) is directly proportional to the acoustic pressure amplitude (P_A), as expressed in Eq. (12):

$$I = \frac{P_A^2}{2\rho c} \qquad (12)$$

where c is the ultrasound speed.

An elevation in the ultrasound intensity raises the acoustic pressure amplitude. This in turn lowers the collapse time (τ_m), as per Eq. (9). In addition, the increase in acoustic pressure amplitude augments the maximum temperature (T_{max}) and the maximum pressure (P_{max}) of bubble collapse, as reflected by Eqs. (10) and (11). Consequently, the bubble collapse becomes significantly more violent and quick at a higher ultrasound intensity. It should be noted that the ultrasound intensity cannot increase past a particular critical value. This critical cutoff point can be explained by the fact that at extremely high acoustic pressure amplitudes, the bubbles are very large, although the time available for the bubble collapse during the compression cycle is insufficient [31]. Furthermore, the larger quantity of bubbles generated at a high intensity can trigger a dampening effect and lower the ultrasound efficacy.

2.7.2 Transmembrane pressure and liquid temperature

Equation (9) indicates that a raised external static pressure (P_0) lowers the collapse time. According to Eqs. (10) and (11), the augmentation of the external pressure increases T_{max} and P_{max} at the point of bubble collapse. As a result, raised external pressure will contribute to a more intense and quick cavitational collapse. High external pressure likewise lowers the liquid vapor pressure. This leads to higher ultrasound intensity that is necessary for the initiation of cavitation [25, 29].

Acoustic cavitation also varies with liquid temperature. A greater temperature causes higher liquid vapor pressure (P_v). As a result, the cavitational collapse is not as intense because of the lower T_{max} and P_{max}, as Eqs. (10) and (11) indicate. For the majority of liquids, higher temperatures imply lower viscosity, which in turn enhances the bubble formation. Since viscous liquids are generally sluggish, they do not let the cavitation bubbles to form easily [28].

2.7.3 Liquid feed and bubble gas characteristics

Cavitation bubbles form reasonably well in liquids with low surface tension, low viscosity, and elevated vapor pressure. Higher vapor pressure, however, also allows for a less aggressive bubble collapse, as outlined in Section 3.7.4. The higher quantity of dissolved gases in liquid augments the number of nuclei available for the subsequent growth of cavitation bubbles. On the other hand, the presence of high concentrations of solid particles reduces the acoustic cavitation because of the weakened and scattered of ultrasonic waves [25, 29].

The overall intensity of cavitational collapse is contingent on the specific heat ratio of the gas located inside the bubble (γ), as shown in Eqs. (10) and (11). Simultaneously, the growth of the gas pressure within the bubble (P_g) causes a less intense cavitational collapse since there is a decrease in T_{max} and P_{max} with P_g, as shown in Eqs. (9) and (10). Thus, gases with lower thermal conductivity generate noticeably higher local heating throughout bubble collapse [28].

3. Influence of ultrasound on membrane fouling remediation

Ultrasound has the capacity to incite critical physical phenomena in heterogeneous solid-liquid systems that can help separate particles from fouled membranes. Ultrasound has been shown to be an effective way in enhancing mass transfer, cleaning, disinfection, and controlling membrane fouling. Some of these relevant physical

phenomena include microstreaming, acoustic streaming, microjets, microstreamers, and shock waves, as shown in **Figure 4**. For instance, acoustic streaming is a type of fluid flow that is caused by the absorption of acoustic, or ultrasonic, energy and does not necessitate a cavitational collapse [31]. When the ultrasonic waves propagate, the wave momentum is absorbed by the liquid. As a consequence, unidirectional flow currents are formed within the liquid [29]. Acoustic streaming produces a low flow velocity of about 10 cms^{-1} and happens within a few centimeters of the ultrasonic transducer [29]. The flow velocity becomes greater at higher ultrasound frequencies and increased power intensity. When it is near a solid surface, including the surface
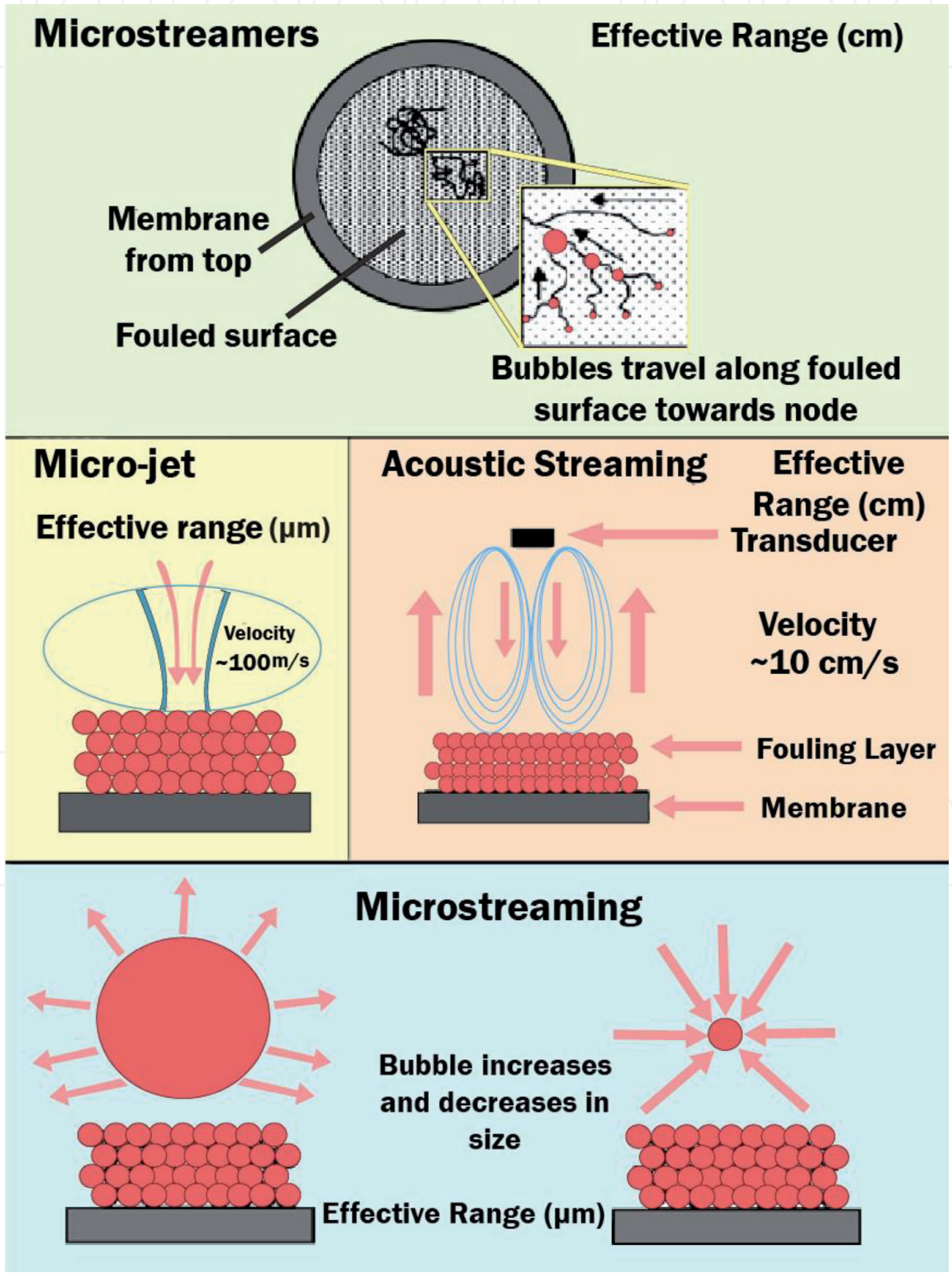

Figure 4.
Influence of ultrasonic on membrane fouling and mechanisms for particle removal/detachment.

of a fouled membrane, the liquid flow generated by acoustic streaming is blocked, causing unidirectional flow parallel to the solid surface that could potentially detach the foulants. Microstreaming is the time-dependent oscillation of liquid molecules located in near the acoustically oscillating cavitation bubbles. Under rarefaction and compression cycles, the oscillation of the cavitation bubbles instigates quick fluctuations in the liquid movement direction and magnitude. Throughout the compression cycle, the cavitation bubbles continue to shrink, while the liquid molecules are moved away from the membrane's surface. Alternatively, in the rarefaction cycle, the cavitation bubbles swell, and the liquid is pushed in the direction of the membrane's surface. The intent is to generate sufficient drag or shear forces that would be able to effectively remove foulants from the membrane's surface. The range of microstreaming effectiveness is relatively limited and generally within the range of 1–100 μm [26, 31]. Microstreamers are produced as a consequence of standing waves created due to the superimposition of the ultrasonic waves redirected from the solid membrane surface and the incoming ultrasonic waves from the ultrasonic transducer. Because of the Bjerknes forces, cavitation bubbles with sizes less than the resonance size are drawn to the standing waves' antinodes. However, cavitation bubbles featuring sizes greater than the resonance size are collected at the nodes. The cavitation bubbles follow a torturous path, forming ribbon-like structures and merging when they come in contact with one another as they move toward the antinodes [26]. In this case, the operational range of microstreamers is several millimeters, and the velocity is around one order of magnitude greater than the average liquid velocity value [30]. It has been shown that microstreamers are involved in detaching foulants from the membrane surface when the antinodes on the membrane surface attract the cavitation bubbles [26, 30]. In a supplement to microstreamers, the appearance of microjets is vital for the release of particles from a fouled membrane. Microjets are created due to the asymmetric cavitation. The liquid movement the vicinity the cavitation bubbles decreases once they are near a solid membrane surface. This in turn produces a differential pressure around the bubbles and a loss of the spherical bubble geometry [30]. Because of the differential pressure, the bubbles tend to discharge strong water jets when they collapse. The microjet's velocity is usually 100–200 ms^{-1}, where the effectual range is in the order of the bubble diameter [31]. Due to the impact of high velocity, microjets can offer a useful capacity for the removal of foulants through erosion and pitting [26]. Lastly, the shock waves produced using ultrasound are critical for the removal of particles from fouled membranes. Throughout rarefaction and compression cycles, shock waves are constantly being generated. Toward the end of compression cycle, the cavitation bubbles abruptly stop once they obtain to their minimum size. At this point, the liquid molecules progressing in the direction of the bubbles are reflected, and this creates high pressure shock waves in the direction of the membrane's surface [25].

3.1 Ultrasound influence on flux improvement and fouling control in wastewater treatment applications

The application of ultrasound for flux improvement in MF and UF processes has been comprehensively investigated. Despite this, research studies linked to ultrasound-assisted flux improvement in NF, MD, FO, RO, and anaerobic membrane bioreactor (AMBR) are currently lacking. Flux improvement related to ultrasound application can be attributed to several key factors. It should be noted that lower-frequency ultrasound reduced the total fouling resistance (R_{tot}) and the reversible fouling resistance (R_{rev}) of polyethersulfone (PES) membrane with dextran feed solution, even with a dead-end UF cell [32]. Lower resistance was linked to a decline in concentration polarization effect because of the cavitation and acoustic streaming generated by ultrasound. As a consequence, when comparing with the flux generated

without ultrasound application, the flux at a transmembrane pressure of 0.4 bar was 83 and 33% larger with ultrasound at frequencies of 28 and 45 kHz, respectively. In this study, the irreversible membrane fouling was insignificant. Reductions in reversible and irreversible fouling in cross-flow UF of clay solution, using hollow fiber polysulfone (PS) membrane, were observed at suitable lower ultrasound frequencies [33]. Since there was a reduction in the fouling resistance, at a transmembrane pressure of 175 kPa, a flux improvement of 33% was attained with the aid of ultrasound at 40 kHz. Furthermore, ultrasound has the potential to lower the filtration resistance in AMBR processes [34, 35]. A number of studies have ascribed flux improvement to acoustic streaming and higher turbulence potential [36–38]. For instance, with dextran feed solution, the flux improvement in the UF process was suggested to be due to the acoustic streaming generated by low-frequency ultrasound.

On the other hand, other study indicated that the application of ultrasound did not offer substantial reduction of internal fouling or pore blockage. Furthermore, it was also noted that the use of ultrasound had little to no influence on pore blocking and adsorption of foulant onto hollow fiber in PS UF membranes. In most instances, whenever the membrane was close to the acoustic cavitation zone, the flux was improved by the collaborative elements of acoustic streaming, microjets, microstreaming, and shock waves. It should be noted that external to the acoustic cavitation zone, increased turbulence and acoustic streaming are the primary influencing factors on the flux improvement [37]. In addition, the implementation of ultrasound in ultrafiltration of water containing 1 mM KCl, and 10 mg/L sulfate latex particles acting as foulants, the ratio of final flux (after the duration of 4 hours) to the initial flux was 0.85 and 0.92, respectively, for applied powers of 0.8 W and 3.3 W [39]. This indicates that the negative influences of fouling were practically eliminated. In a study of inorganic fouling of commercial polyamide-based RO membranes using a $CaSO_4$ solution, the effects of microstreaming in the membrane pores and on the membrane surface were believed to be the primary reason behind membrane cleaning and the flux enhancement obtained [40]. In general, for an experimental duration of 3 h, the permeate flux increased by about 50.8% for the 500 mg/L $CaSO_4$ solution and 69.7% for the 1000 mg/L $CaSO_4$ solution with the application of the 20 kHz ultrasound, as compared with the runs without ultrasound. The ultrasound irradiation could likewise improve the flux through the agglomeration of small particles, thus lowering the chances of pore blockage. In ultrafiltration of wastewater using PS hollow fiber membrane, an agglomeration of small suspended particles was detected because of the vibration and microstreamers. The agglomeration that occurs when the ultrasound was used resulted in a greater turbidity removal, compared to the turbidity removal when ultrasound was not employed.

Choi et al. also used 72 kHz ultrasound to lower silica colloidal fouling and calcium sulfate scaling in a commercial cellulose acetate FO membrane [41]. Ultrasound appeared to disassemble silica colloids and calcium sulfate crystals in the feed solution. In terms of flux improvement, the ultrasound-assisted FO (UAFO) process was much more successful than FO. In comparison to FO processes, the initial flux with UAFO was about 25% higher, and 166% higher with calcium sulfate scaling. For silica colloidal type fouling, permeate flux decrease was only 21% for FO, compared to 50% flux drop with FO without ultrasound. The ultrasound-assisted flux improvement during FO filtration of tannin using a thin-film composite (TFC) membrane was also examined. The flux improvement was caused by the lessening of concentration polarization in the membrane's porous support layer [42]. In addition, the reverse salt flux was greater whenever ultrasound was applied. Also, ultrasound was found relevant for the mitigation of silica colloid and calcium sulfate fouling during the membrane distillation (MD) process. In a research study on the effects of ultrasound on the performance of MD, the specific ratio of fouled-membrane flux to the initial flux was

upheld at 93 and 97% with calcium sulfate and silica fouling, respectively, because of the microstreaming and shock waves generated by the ultrasound [43].

3.2 Ultrasound influence on fouling control in protein separation/purification downstream processing

The concentration polarization occurs when a concentration gradient of the protein is formed on or near the membrane surface. Similarly, this phenomenon is predominantly a function of membrane hydrodynamics. Conversely, fouling is the result of accumulation of proteins drawn toward filtering surface by convective flow of filtrate through the membrane. Membrane cleaning is significantly enhanced by cavitation and acoustic streaming induced by ultrasonic waves. Ultrasound generates acoustic streaming and cavitation bubbles in a liquid medium. Cavitation bubbles cause microstreaming, microstreamers, microjets, and shock waves, as described in **Figure 4**. Acoustic streaming and shear forces imposed by cavitation bubbles reduce protein fouling on the membrane surface. This leads to an increase in permeate flux. Several mechanisms of protein release from a protein-fouled surface by the effects of ultrasound were proposed, as presented in **Figure 4** for the removal/detachment mechanisms. Acoustic streaming does not require the collapse of cavitation bubbles, and it was defined as the absorption of acoustic energy resulting in fluid flow [44]. This protein removal mechanism is expected to be important near surfaces with loosely attached particles or with readily dissolvable surfaces. Higher frequency ultrasound tends to have higher energy absorption by liquid and thus greater acoustic streaming flow rates than lower frequencies at the same power intensity [45]. In addition, higher power intensities lead to greater acoustic streaming flow rates due to higher energy gradients in liquid between acoustically and nonacoustically stimulated areas. Acoustic streaming causes bulk water movement toward and away from the membrane cake layer, with velocity gradients near the protein cake layer that may scour proteins from the surface. The effect of ultrasound on the flux and solute rejection in cross-flow UF of BSA-lysozyme binary protein mixture, using PES membrane (30 kDa MWCO), was investigated and reported [44, 45]. The authors observed that ultrasonic wave not only enhanced the UF flux but also increased the lysozyme rejection. Particularly, at ultrasound wave of 25 kHz and 240 W, increases in UF flux of 135 and 120% were obtained with PES membrane at pH of 11 in the upward and downward modes, respectively, in contrast to the case without ultrasound [44, 45]. Enhanced flux in continuous UF processes was achieved with an interrupted ultrasound, and more hydrophilic ultrafilter membranes in the upward operating mode were achieved [46]. It was noticed that the effectiveness of ultrasound in membrane protein purification depends on many factors, such as orientation and position of ultrasonic field, ultrasonic frequency and power, ultrasonic radiation angle, position of ultrasonic vibration plate in the membrane module, membrane material, membrane housing, operating pressure, and the fouling material. It was widely believed that ultrasonic cavitation, acoustic streaming, ultrasonic-induced vibration of membrane, and ultrasonic heating were the main causes for the enhanced separation performance and permeate flux [44]. Electric and ultrasonic fields can reduce membrane fouling and in turn of enhanced flux, when both the fields were applied simultaneously [47]. Both electric and ultrasonic fields reduced the fouling when applied individually, but the extent of improvement by the ultrasonic field could be minimal. The improvement by the electric field is invariably considerably greater than that due to the ultrasonic field, particularly when the proteins are well dispersed (high zeta potential).

In another case study examined the filtration of whey solution, using a PS membrane and a cross-flow UF apparatus, the flux improvement was primarily caused by the mechanical vibrations and acoustic streaming instead of the acoustic

cavitation. For shorter filtration times, the decline of the permeate flux was caused by the pore blockage. On the other hand, the decline in flux was controlled by the growth of cake layer with longer filtration times. Ultrasound lowered the resistance of the initial deposit layer and the growing cake layer [26]. The specific ratio of the steady flux with ultrasound in comparison to the steady flux without ultrasound was determined at about 1.2 and 1.7 throughout the complete experimental range.

3.3 Fouled membrane cleaning and flux restoration

Ultrasound can be effectively used for cleaning fouled membranes. A number of researchers have explored the use of ultrasound as a potential membrane cleaning method. Ultrasound-assisted cleaning of membranes may be conducted in different ways. For instance, the membrane can be cleaned in an ultrasonic cleaning bath or, alternatively, washed online in a filter using cleaning chemicals or washed with water while applying ultrasound irradiation. In a reported study, Anodisc™ γ-Al$_2$O$_3$ ceramic membrane was exposed to ultrasound inside a closed washing vessel containing water [39]. The membranes were specifically fouled with sulfate polystyrene latex particles. Once the external cleaning was performed, a complete retrieval of clean water flux was detected for all frequencies, with the exception of 1062 kHz, since the ultrasonic treatment time and power intensity were higher than 30 s and 1.05 W cm^{-2}. In addition, an exterior ultrasonic cleaning vessel using a 1 mM KCl solution was used to wash the Anodisc™ γ-Al$_2$O$_3$ ceramic and polyvinylidene difluoride (PVDF) membranes [39]. It was reported that the membranes were almost completely washed, while the water flux after washing was near the original level of clean water flux in new membranes. In a different study, cellulose MF and PS UF membranes were washed inside a filtration cell using a combination of ultrasound and water washing [48].The cellulose and PS membranes were initially fouled using milk solution and peptone solution. Complete and partial washing for the PS and the cellulose membrane was obtained at 28 kHz, respectively. Similar membrane washing procedures have also been used in other research studies [49, 50]. Different ways of cleaning nylon MF membrane that were fouled using Kraft paper mill effluent were comparatively examined. The experimental results obtained suggest that the washing efficacy was best (97.8%) when ultrasound was implemented in conjunction with forward flushing. Several studies combining EDTA chelating agent and ultrasound were carried out to clean fouled spiral wound PES membranes in ultrafiltration of skimmed milk solution. A synergistic effect was detected when EDTA and ultrasound were simultaneously applied. The best cleaning was noted when 3 mM EDTA and ultrasound mixed waveform were applied simultaneously. Furthermore, it was stated that a 5-minute period of forward flushing with ultrasound and sequestering agent EDTA was sufficient for membrane cleaning without supplementary washing. Comparable experimental results were obtained, where synergistic outcome was perceived in cases where the ultrasound was applied together with EDTA during cleaning of PVDF MF membranes fouled with a 1% milk solution [51].

4. Challenges in industrial applications of ultrasound

Although research has shown the efficacy of ultrasound as a method to improve membrane cleaning and flux, hands-on ultrasound applications in membrane-dependent separation processes still have a number of critical challenges. One such issue is associated with membrane damage. When exposed to ultrasound, the membranes can become vulnerable to damage due to the intense cavitational collapse contingent on the power density, frequency, and the irradiation time of ultrasound.

A number of research studies have offered examples of membrane integrity loss and membrane damage due to ultrasound exposure [45, 52, 53]. The ultrasound power intensity needs to be carefully coordinated so as to minimize energy consumption and potential membrane damage. An in-depth study on the influences of 47 kHz ultrasound on polymeric membranes was conducted. During this experiment, three polymeric membrane were used: PES (MWCO: 3, 10, 30, and 100 kDa), PVDF (MWCO: 40 kDa), and polyacrylonitrile (PAN; MWCO: 40 and 50 kDa). Once a 2-hour ultrasonic treatment was completed, PES membranes were affected over the entire surface area, while PVDF (40 kDa) and PAN (50 kDa) were influenced on the edge areas. Except for PAN (40 kDa), other membranes showcased significant differences in their water permeability, with membrane degradation occurring primarily within the first 5 min of exposure to ultrasound. A research study examined the effect of 40 kHz ultrasound on polymeric MF membranes [53]. The membranes used included mixed ester of cellulose nitrate and cellulose acetate (CN-CA), PES, nylon 6 (N6), and PVDF. Except for PVDF membranes, at a power intensity of 2.13 W/cm^2, all membranes used showed partial damage that caused an increase in water flux after 60 min of ultrasound session. PVDF membrane had some damage only at a power intensity of 3.7 W/cm^2 after a 90-min exposure. Another study likewise confirmed some impairment to ceramic Anodisc™ γ-Al$_2$O$_3$ membranes after a sonication of 20 kHz for 5 min [39]. Membrane damage took the form of pitting on the membrane surface, which was caused by microjets and shock waves. Alternatively, it was found that PVDF hollow fiber UF membranes were damaged by ultrasound at 8.68 kW/m^2 within 6 min of exposure [54]. The number of research studies focused exclusively on ultrasound-induced membrane damage is relatively low. There is a lack of research on membrane materials that can offer a range of resistance potential against damage incurred by ultrasonic treatment. Consequently, further research is necessary for the proper assessment of the effects of ultrasound on the integrity of membranes consisted of diversified materials. Another key challenge that needs to be addressed is related to the industrialization of ultrasound-assisted membrane process. The vast majority of all research studies on the application of ultrasound to membrane cleaning and flux improvement have been done with laboratory-scale cross-flow units. Although there are a high number of such ultrasound studies, effective commercial application of ultrasound technology requires further in-depth case studies with large-scale membrane process; these, however, are currently not available. New research investigations must be conducted on the relevance of ultrasound in cleaning of full-scale membrane modules. There is a common agreement in scientific research community that ultrasound is a highly encouraging method for membrane cleaning and flux improvement; however, the economic value and industrial application feasibility are still challenges that must be addressed. Contingent on the real-life operating conditions, the power requirements of ultrasound could be so high as to constraint its applicability on an industrial scale. Currently, there has been no study on the specific economics behind membrane-based, ultrasound-assisted, or membrane cleaning process types. Thus, the economic viability of ultrasound-assisted membrane cleaning and flux improvement demands urgent response. The exact source of ultrasound likewise poses another issue when it comes to the effective applications of ultrasound in large-scale membrane processes. In general, research studies have been dependent on the usage of probes, horns, or ultrasonic baths. Due to their limitations, all of these ultrasound sources will most likely to be ineffectual in large-scale applications. As a result, research into ultrasound transducer technologies is becoming essential. Additional experimental work is necessary for the examination of the success of ultrasound in flux improvement and washing processes for diverse membrane module types. The majority of research studies have concentrated on flat

sheet membranes, and only a small number of studies on spiral wound or hollow fiber membranes, for which the ultrasound applications are much more strenuous due to membrane configuration. Another research gap is in the understanding of the effects of ultrasound on cleaning and flux improvement in membrane processes other than UF and MF. The absence of these critical research studies is a difficult challenge for future implementation of ultrasound-assisted membrane processes on a larger industrial scale.

5. Conclusion

This review paper recapitulates some of the critical research efforts currently being made toward effective ultrasound-assisted membrane cleaning and flux improvement. As the experimental outcomes reviewed in this chapter suggest, ultrasound, including continuous and intermittent waves, is an efficient method of flux improvement, membrane fouling minimization, and membrane cleaning because it has a distinctive capability to produce unique physical and chemical effects that can successfully remove foulants from the membrane surface. Despite these advantages, ultrasound application cannot significantly deter pore blockages and is limited to external fouling. Although it is an effective method for membrane cleaning and flux improvement in wastewater treatment and protein purification downstream processing, ultrasound-assisted membrane technology is still in its developmental stages due to a number of key limitations. The primary issues preventing a more effective use of ultrasound-assisted membrane technology include concerns about installation in large-scale systems, absence of suitable transducers, and scarcity of relevant data on its economic feasibility. In addition, mathematical concepts and model descriptions are needed to understand membrane fouling and permeate flux as a function of ultrasonic parameters. Substantial research enquiries are necessary for further analysis and remediation of membrane damage by ultrasound, the efficacy of ultrasound applications for membranes other than those of the flat-sheet type, and the economics of the ultrasound-assisted membrane process.

Nomenclature

λ (m)	wavelength of one pressure oscillation
f (Hz)	frequency of the ultrasound wave, which is the number of pressure oscillations per unit time, and the inverse of the time period of one oscillation
f_b (Hz)	bubble oscillation frequency
c (m/s)	ultrasound speed, which is the distance of wave propagation per unit time [ultrasound speed = frequency × wavelength, $(c = f\lambda)$]
P (W)	power of ultrasound wave, which is the time rate of the energy of ultrasound passing through a surface perpendicular to the direction of the wave propagation
I (W/m^2)	intensity of ultrasound wave, which is the ultrasonic energy passing a unit surface perpendicular to the direction of wave propagation per unit time
P_a (Pa)	acoustic pressure, which is the pressure created as a result of compression or rarefaction zones relative to the fluid hydrostatic pressure
P_A (Pa)	acoustic pressure amplitude, which is the maximum height of the ultrasonic wave

P (Pa)	pressure inside the bubble at the maximum radius value [$P = P_v$ (vapor pressure) + P_g (gas pressure)]
P_m (Pa)	liquid pressure at the transient collapse moment [$P_m = P_0 + P_A$]
$P\infty$ (Pa)	pressure value at an infinite distance away from the bubble
Po (Pa)	hydrostatic pressure being applied on the liquid or pressure value close to the bubble
P_{max} (Pa)	maximum pressure
Pb (pa)	Blake threshold pressure
ω (Hz)	ultrasound's angular frequency
γ (unitless)	specific gas heat ratio within the bubble
ρ (Kg/m^3)	liquid density
μ (cP)	liquid viscosity
σ (N/m)	liquid's surface tension
R_0 (m)	cavitation bubble of initial radius
R_{max} (m)	maximum bubble radius before the collapse
R (m)	bubble radius
R_r (m)	bubble's resonance size, which is a function of ultrasound frequency
T_a (s)	time period of one oscillation
t (s)	time
τ_m (s)	bubble collapse time
T_{max} (K)	maximum temperature of the feed

Acknowledgements

Author details

Amira Abdelrasoul[1]* and Huu Doan[2]

1 Department of Chemical and Biological Engineering, Division of Biomedical Engineering, University of Saskatchewan, Saskatoon, Saskatchewan, Canada

2 Department of Chemical Engineering, Ryerson University, Ontario, Canada

*Address all correspondence to: amira.abdelrasoul@usask.ca

IntechOpen

References

[1] Abdelrasoul A, Doan H, Lohi A, Cheng C-H. Membrane fouling control & performance enhancement of ultrafiltration of latex effluent. The Canadian Journal of Chemical Engineering. 2016;**94**:281-290

[2] Abdelrasoul A, Doan H, Lohi A. Membrane fouling remediation in ultrafiltration of latex contaminated water and wastewater. Water Quality Research Journal of Canada. 2015;**51**(3):256-269

[3] Abdelrasoul A, Doan H, Lohi A. A mechanistic model for ultrafiltration membrane fouling by latex. Journal of Membrane Science. 2013;**433**:88-99

[4] Abdelrasoul A, Doan H, Lohi A. Impact of operating conditions on fouling probability and cake height in ultrafiltration of latex solution. Journal of Membrane and Separation Technology. 2013;**2**:134-147

[5] Ciu Z. Protein separation using ultrafiltration—An example of multi-scale complex systems. China Particuology. 2005;**3**(6):343-348

[6] Abdelrasoul A, Doan H, Lohi A, Cheng C-H. Innovative membrane technology: Predicting power consumption and performance in ultrafiltration of simulated latex effluent using non-uniform pore size membranes. Korean Journal of Chemical Engineering. 2016;**33**(3):1014-1027

[7] Abdelrasoul A, Doan H, Lohi A, Cheng C-H. Morphology control of polysulfone membranes in filtration processes: A critical review. ChemBioEng Reviews. 2015;**2**(1):22-43

[8] Abdelrasoul A, Doan H, Lohi A, Cheng C-H. The effect of contaminated particle sphericity and size on membrane fouling in cross flow ultrafiltration. Environmental Technology. 2018;**39**(2):203-220

[9] Abdelrasoul A, Doan H, Lohi A, Cheng C-H. Contaminated particle characteristics influence on membrane fouling. Water Environment Journal. 2017;**31**(1):31-38

[10] Abdelrasoul A, Doan H, Lohi A, Cheng C-H. The influence of aggregation of latex particles on membrane fouling attachments & ultrafiltration performance in ultrafiltration of latex contaminated water and wastewater. Journal of Environmental Sciences. 2017;**53**:118-129

[11] Abdelrasoul A, Doan H, Lohi A, Cheng C-H. Modeling of fouling and fouling attachments as a function of the zeta potential of heterogeneous membranes surfaces in ultrafiltration of latex solution. Industrial & Engineering Chemistry Research. 2014;**53**:9897-9908

[12] Abdelrasoul A, Doan H, Lohi A, Cheng C-H. Modeling of fouling and foulant attachments on heterogeneous membranes in ultrafiltration of latex solution. Separation and Purification Technology. 2014;**135**:199-210

[13] Abdelrasoul A, Doan H, Lohi A. Effect of pH on fouling attachments and power consumption in ultrafiltration of latex solution. The Canadian Journal of Chemical Engineering. 2014;**92**(7):1293-1305

[14] Abdelrasoul A, Doan H, Lohi A, Cheng C-H. Modeling development for ultrafiltration membrane fouling of heterogeneous membranes with non-uniform pore size. The Canadian Journal of Chemical Engineering. 2014;**92**(11):1926-1938

[15] Kang J, Du G, Gao X, Zhao B, Guo J. Soluble microbial products from

water biological treatment process: A review. Water Environment Research. 2014;**86**(3):223-231

[16] Uyak V, Akdagli M, Cakmakci M, Koyuncu I. Natural organic matter removal and fouling in a low pressure hybrid membrane systems. The Scientific World Journal. 2014;**2014**:893203-893214

[17] Li Q, Elimelech M. Organic fouling and chemical cleaning of nanofiltration membranes: Measurements and mechanisms. Journal of Environmental Science and Technology. 2004;**38**(17):4683-4693

[18] Amy G. Fundamental understanding of organic matter fouling of membranes. Desalination. 2008;**231**(1-3):44-52

[19] Shirazi S, Lin C, Chen D. Inorganic fouling of pressure-driven membrane processes—A critical review. Desalination. 2010;**250**(1):236-248

[20] Han G, Zhou J, Wan C, Yang T, Chung T. Investigations of inorganic and organic fouling behaviors, antifouling and cleaning strategies for pressure retarded osmosis (PRO) membrane using seawater desalination brine and wastewater. Water Research. 2016;**103**:264-275

[21] Abdelrasoul A, Doan H, Lohi A. Fouling in membrane filtration and remediation methods. In: Nakajima H, editor. Mass Transfer—Advances in Sustainable Energy and Environment Oriented Numerical Modeling. Vol. 8. London, UK: Intech Open Access Publisher; 2013. pp. 195-218

[22] Nguyen T, Roddick F, Fan L. Biofouling of water treatment membranes: A review of the underlying causes, monitoring techniques and control measures. Membranes. 2012;**2**:804-840

[23] Yasui K. Acoustic Cavitation and Bubble Dynamics. 1st ed. Cham: Springer International Publishing; 2018. DOI: 10.1007/978-3-319-68237-2

[24] Luo L, Fang Z, Smith RL, Qi X. Fundamentals of acoustic cavitation in sonochemistry. In: Fang Z, Smith RL Jr, Qi X, editors. Production of Biofuels and Chemicals with Ultrasound. 1st ed. Dordrecht: Springer Science; 2015. pp. 3-33

[25] Lorimer JP, Mason TJ. Sonochemistry. Part 1—The physical aspects. Chemical Society Reviews. 1987;**16**:239-274

[26] Muthukumaran S, Kentish S, Stevens G, Ashokkumar M. Application of ultrasound in membrane separation processes: A review. Reviews in Chemical Engineering. 2006;**22**:155-194

[27] Wu TY, Guo N, Teh CY, Hay J. Theory and fundamentals of ultrasound. In: Advances in Ultrasound Technology for Environmental Remediation. Dordrecht: Springer; 2013. pp. 5-12. DOI: 10.1007/978-94-007-5533-8

[28] Pang YL, Abdullah AZ, Bhatia S. Review on sonochemical methods in the presence of catalysts and chemical additives for treatment of organic pollutants in wastewater. Desalination. 2011;**277**:1-14

[29] Lamminen M, Walker H, Weavers L. Mechanisms and factors influencing the ultrasonic cleaning of particle-fouled ceramic membranes. Journal of Membrane Science. 2004;**237**:213-223

[30] Adewuyi Y. Sonochemistry: Environmental science and engineering applications. Industrial and Engineering Chemistry Research. 2001;**40**:4681-4715

[31] Pham M, Shrestha T, Amatya R. Ultrasound Technology in Green

Chemistry. Dordrecht: Springer; 2011. DOI: 10.1007/978-94-007-2409-9

[32] Cai M, Zhao S, Liang H. Mechanisms for the enhancement of ultrafiltration and membrane cleaning by different ultrasonic frequencies. Desalination. 2010;**263**:133-138

[33] Li X, Yu J, Nnanna A. Fouling mitigation for hollow-fiber UF membrane by sonication. Desalination. 2011;**281**:23-29

[34] Sui P, Wen X, Huang X. Feasibility of employing ultrasound for on-line membrane fouling control in an anaerobic membrane bioreactor. Desalination. 2008;**219**:203-213

[35] Xu M, Wen X, Huang X, Yu Z, Zhu M. Mechanisms of membrane fouling controlled by online ultrasound in an anaerobic membrane bioreactor for digestion of waste activated sludge. Journal of Membrane Science. 2013;**445**:119-126

[36] Chen D, Weavers L, Walker H. Ultrasonic control of ceramic membrane fouling: Effect of particle characteristics. Water Research. 2006;**40**:840-850

[37] Chen D, Weavers L, Walker H. Ultrasonic control of ceramic membrane fouling by particles: Effect of ultrasonic factors. Ultrasonics Sonochemistry. 2006;**13**:379-387

[38] Chen D, Weavers L, Walker H. Ultrasonic control of ceramic membrane fouling caused by natural organic matter and silica particles. Journal of Membrane Science. 2006;**276**:135-144

[39] Lamminen MO, Walker HW, Weavers LK. Cleaning of particle-fouled membranes during cross-flow filtration using an embedded ultrasonic transducer system. Journal of Membrane Science. 2006;**283**:225-232

[40] Feng D, van Deventer J, Aldrich C. Ultrasonic defouling of reverse osmosis membranes used to treat wastewater effluents. Separation and Purification Technology. 2006;**50**:318-323

[41] Choi YJ, Kim SH, Jeong S, Hwang TM. Application of ultrasound to mitigate calcium sulfate scaling and colloidal fouling. Desalination. 2014;**336**:153-159

[42] Heikkinen J, Kyllönen H, Järvelä E, Grönroos A, Tang CY. Ultrasound-assisted forward osmosis for mitigating internal concentration polarization. Journal of Membrane Science. 2017;**528**:147-154

[43] Hou D, Wang Z, Li G, Fan H, Wang J, Huang H. Ultrasonic assisted direct contact membrane distillation hybrid process for membrane scaling mitigation. Desalination. 2015;**375**:33-39

[44] Saxena A, Tripathi BP, Kumar M, Shahi V. Membrane-based techniques for the separation and purification of proteins: An overview. Advances in Colloid and Interface Science. 2009;**145**:1-2

[45] Marcet I, Salvadores M, Rendueles M, Díaz M. The effect of ultrasound on the alkali extraction of proteins from eggshell membranes. Journal of the Science of Food and Agriculture. 2018;**98**(5):1765-1772

[46] Teng M, Lin S, Juang R. Effect of ultrasound on the separation of binary protein mixtures by cross-flow ultrafiltration. Desalination. 2006;**200**(1-3):280-282

[47] Avrahami R, Rosenblum J, Gazes M, Rosenblum S, Litman L. The effect of combined ultrasound and electric field stimulation on wound healing in chronic ulcerations. Wounds. 2015;**27**(7):199-208

[48] Kobayashi T, Kobayashi T, Hosaka Y, Fujii N. Ultrasound-enhanced membranecleaning processes applied water treatments: Influence of sonic frequency on filtration treatments. Ultrasonics. 2003;**41**:185-190

[49] Muthukumaran S, Yang K, Kentish S, Ashokkumar M, Stevens GW. The use of ultrasonic cleaning for ultrafiltration membranes in the dairy industry. Separation and Purification Technology. 2004;**39**:99-107

[50] Lu JY, Du X, Lipscomb G. Cleaning membranes with focused ultrasound beams for drinking water treatment. In: IEEE International Ultrasonics Symposium. 2009. pp. 1195-1198

[51] Maskooki A, Kobayashi T, Mortazavi S, Maskooki A. Effect of low frequencies and mixed wave of ultrasound and EDTA on flux recovery and cleaning of microfiltration membranes. Separation and Purification Technology. 2008;**59**:67-73

[52] Masselin I, Chasseray X, Durand-Bourlier L, Lainé JM, Syzaret PY, Lemordant D. Effect of sonication on polymeric membranes. Journal of Membrane Science. 2001;**181**:213-220

[53] Wang X, Li X, Fu X, Chen R, Gao B. Effect of ultrasound irradiation on polymeric microfiltration membranes. Desalination. 2005;**175**(2005):187-196

[54] Jin W, Guo W, Lü X, Han P, Wang Y. Effect of the ultrasound generated by flat plate transducer cleaning on polluted polyvinylidenefluoride hollow fiber ultrafiltration membrane. Chinese Journal of Chemical Engineering. 2008;**16**:801-804